Cold atomic clouds and Bose-Einstein condensates passing through a Gaussian beam

Shuyu Zhou,[1] Zhenglu Duan,[2] Jing Qian,[2] Zhen Xu,[1] Weiping Zhang,[2,*] and Yuzhu Wang[1,†]
[1]*Key Laboratory for Quantum Optics, Shanghai Institute of Optics and Fine Mechanics, The Chinese Academy of Sciences, Shanghai 201800, China*
[2]*State Key Laboratory of Precision Spectroscopy, Department of Physics, East China Normal University, Shanghai 200062, China*

(Received 23 February 2009; revised manuscript received 5 June 2009; published 14 September 2009)

We have experimentally studied and numerically simulated the behavior of cold atomic clouds and Bose-Einstein condensates passing through a far red-detuned Gaussian beam. Several exotic phenomena such as the focusing and advancement of atomic clouds have been exhibited. The cooling effect and the effective interaction length of the dipole potential to the atoms have also been discussed.

DOI: 10.1103/PhysRevA.80.033411 PACS number(s): 37.10.De, 37.10.Vz

I. INTRODUCTION

Currently, laser cooling and evaporative cooling techniques have made it easy to obtain ultracold atomic clouds and Bose-Einstein condensates (BECs) at the temperature order of 100 nK [1–3]. This kind of ultralow temperature atomic cloud is suitable as a medium in atom optics studies [4,5]. Especially for BECs, the macroscopical atomic wave packet easily exhibits wave characteristics such as interference and diffraction [6–9]. Several kinds of atom-optical elements have been developed. Reflection and focusing have been achieved through magnetic mirrors and lenses [10–12]. The focusing dynamics have also been investigated; specifically, the isotropic three-dimensional (3D) focusing of atoms with a single-impulse magnetic lens [13]. Atom-optical elements based on magnetic fields are advantageous for coherent atom-optic research owing to their extremely high optical quality. However, it is difficult to build flexible optical systems because magnetic atom-optical elements have a large scale. Laser beams are often used to build atomioptical elements because of their interaction with atoms [14]. They have a small scale and are scalable. For example, atom-optical lenses can be achieved through red-detuned Gaussian beams or blue-detuned doughnut beams [5,15–19], atomic mirrors made by nonuniform laser wave fields [20], and gratings constructed by standing waves [21]. There are other ways to achieve an atom-optical lens, such as through the use of radiation-pressure force [22,23], near-field light [24,25], and far-detuned and resonant standing wave fields [26]. It is easy to obtain Gaussian beams in experiments. If the frequency detuning is negative (i.e., red detuning), then the dipole force is toward the maximum intensity region. Hence, a focused Gaussian laser beam with red detuning can be used as an atom-optical lens. Early experiments demonstrated this kind of atomic beam focusing using the dipole force [5,15,16,27,28]. The focusing dynamics of a trapped BEC interacting with laser pulses have also been investigated [29]. Aberration-free atom-optical lenses based on the optical dipole force have also been proposed [30,31]. Recently, an increasing number of research groups have shown interest in standing wave optical diffraction grating [32], that is, the optical lattice, a lensing effect that has also been observed by experimentalists [33]. Released atoms from a magneto-optical trap (MOT) guided by a red-detuned Gaussian beam have also been investigated. Heating and cooling effects caused by an adiabatic compression and expansion when the cold atomic cloud is close to or far from the focus of the Gaussian beam, respectively, have likewise been found [34]. However, as far as we know, there has been no report on the study of ultracold atomic clouds (whose temperature is around the Bose-Einstein transition temperature) passing through a Gaussian beam along its radial direction. Low-velocity atomic clouds will be focused within a short distance with the appropriate parameters. If the de Broglie wavelength of the atoms can be compared to the scale of the laser beam, diffraction will happen.

In this paper, we have experimentally studied the behavior of ultracold ^{87}Rb atoms passing through a red-detuned Gaussian beam in gravity. Focusing and cooling in the transverse direction and advances along the motional direction of atomic clouds have been observed. Based on the two-level atom model interacting with a light field, we have performed a numerical simulation, which agrees with the experiment.

II. THEORY AND NUMERICAL SIMULATION

In Fig. 1, we consider a model describing an atomic cloud as it traverses a far red-detuned focused Gaussian laser beam under the gravity field. As shown in the figure, x is the direction of the laser beam's propagation.

Then we study the figure under two conditions. One case is where the temperature of the atomic cloud is higher than the phase transition temperature. All atoms in the atomic cloud are doing thermal motions without correlations with each other. Here, we use the direct simulation Monte Carlo (DSMC) approach [35] to simulate the condition. The other case is where the phase transition has occurred and atoms have accumulated in the quantum state with the lowest energy. We describe this condition via the quantum mechanical method.

A. Cold atomic clouds

When an atomic cloud's temperature is higher than the phase transition temperature, each atom in the cloud does a

*wpzhang@phy.ecnu.edu.cn
†yzwang@mail.shcnc.ac.cn

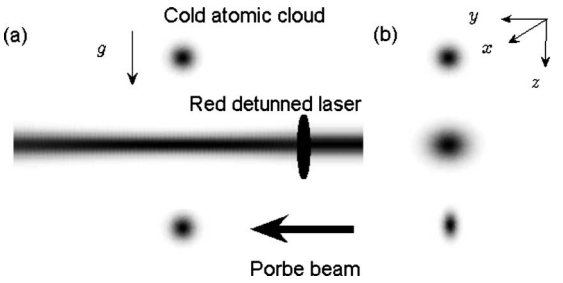

FIG. 1. (a) Experimental setup scheme. An atomic cloud interacts with a red-detuned focused Gaussian light field in the gravity filled while another probe beam plays the role of absorption image in the far field. (b) Cross section. Focusing is observed when the atomic cloud passes the Gaussian filed.

noncorrelative thermal motion. Every atom can be considered as a classical particle moving in an external potential composed by the gravity field and the potential well induced by the laser field

$$V = \frac{\hbar|\Omega(\vec{r})|^2}{4(\delta + i\gamma/2)} + mgz, \tag{1}$$

where m is the mass of the atom, $\Omega(\vec{r})$ describes the dipole coupling of atoms with the laser field, $\delta = \omega_L - \omega_a$ is the detuning between the laser frequency and the transition frequency of the atom, and γ represents the decay rate of the atomic excited state owing to spontaneous radiation. For a focused Gaussian laser beam, the Rabi frequency spatially depends on $\Omega(\vec{r}) = \Omega_0 e^{-((y-y_0)^2+(z-z_0)^2)/w_L^2}$, where Ω_0 is determined by the intensity in the center of the Gaussian beam and w_L is the waist size of the Gaussian beam.

Since there are a large number of atoms in the cold atomic cloud, we use the DSMC approach to simulate it. We assume that the initial position distribution and velocity distribution satisfy the Maxwell-Boltzmann distributions. Considering the collision between atoms, the motion of a thermal atomic cloud can be expressed as an ensemble average of many particles' motional trajectories. In comparison to the following experimental results, the parameters in the simulation are found to be identical with those obtained in the experiments.

The result of the numerical simulation is shown in Fig. 2, in which Fig. 2(a) plots the image of cold atomic clouds with a different initial temperature. It explicitly shows that the atomic cloud has been focused with a background. With the decrease in temperature, the background atomic cloud becomes smaller and smaller, while the number of focused atoms increases. Figure 2(b) presents the corresponding cross curves along the y axis at the widest part of the atomic cloud.

It is interesting to note that there is one-dimension cooling in the direction perpendicular to that of the gravity and light beam (shown in Fig. 3). However, in comparison to the initial velocity distribution along the y and z directions, we find that the one-dimension cooling occurs in the y direction while heating and acceleration occur in the z direction. The sum of kinetic energy and gravitational potential energy of all atoms has no change before and after atomic clouds passing through the Gaussian beam, which ensures the energy

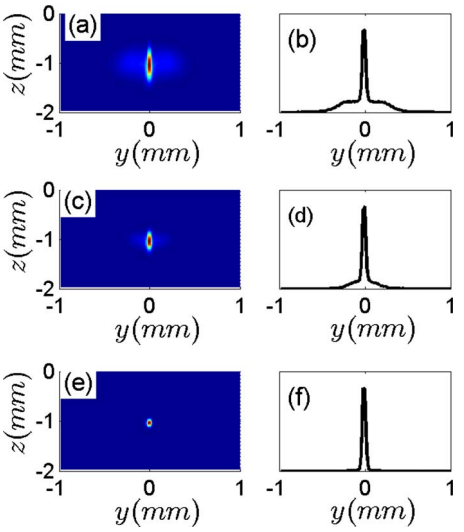

FIG. 2. (Color online) Left panels: Images of the simulated cold atomic clouds after traversing through a red-detuned Gaussian beam. Right panels: Corresponding cross section of the atomic cloud along the y axis at the widest part of the atomic cloud. From top to bottom, the corresponding temperatures are $T=1.5$, 0.48, and 0.08 μK, respectively. Here, the Rabi frequency is $\Omega_0/2\pi = 100$ MHz, the detuning is $\delta/2\pi = -50$ GHz, the waist length $w_L = 46$ μm, the flying time before optical field is $t_1 = 7$ ms, and the flying time after the optical field is $t_2 = 9$ ms.

conservation law. This effect shows that the Gaussian beam plays the role of redistributing kinetic energy of cold atomic clouds.

Figure 4 is the cross curve along the z axis (gravity direction). We find that when the atomic cloud passes through the light beam, there is a spatial advancement comparable to that in free flying. The physical reason for the advance phenomenon can be explained by a classical picture. A focused far red-detuned Gaussian beam corresponds to a potential well. When an atomic cloud traverses it, according to the energy conservation law, the average velocity of atoms is larger than that of freely flying atoms over the same region without laser field. Therefore an advance of atomic cloud in space is exhibited.

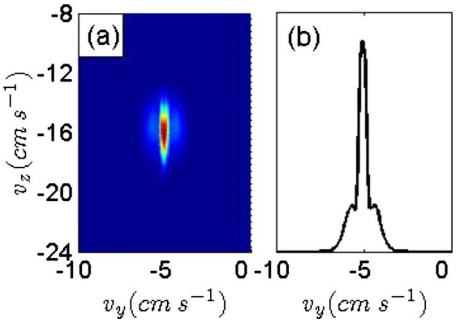

FIG. 3. (Color online) (a) The theoretical velocity distribution in the y-z plane. (b) The velocity distribution along the v_y direction in the cross section of $v_z = 15.68$ cm s^{-1}.

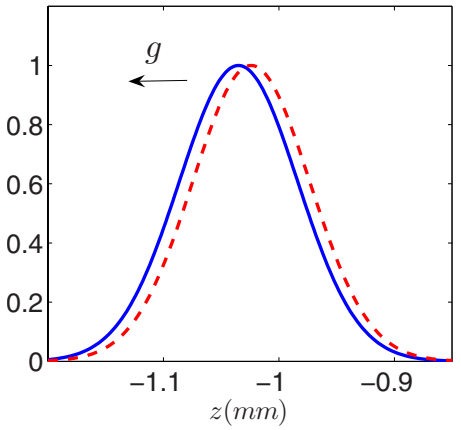

FIG. 4. (Color online) The simulated advance effect along the z direction. The dashed curve plots the cold atomic cloud's freefall in the gravity field, while the solid curve shows the atomic cloud as it traverses through the Gaussian light beam in the gravity field.

B. Bose-Einstein condensates

The atoms in a BEC cannot be distinguished. Thus, it can be expressed by a single wave function. A high-density condensate, in the mean field level, can be described via the nonlinear Schrödinger equation

$$i\hbar\frac{\partial\psi}{\partial t} = -\frac{\hbar^2\nabla^2}{2m}\psi + \frac{\hbar|\Omega(\vec{r})|^2}{4(\delta + i\gamma/2)}\psi + mgz\psi + g_aN|\psi|^2\psi, \tag{2}$$

where $g_a = 4\pi\hbar^2 a_s/m$ is the atom-atom interaction, a_s is the s-wave scattering length, and N is the total number of atoms.

Based on Eq. (2), we performed numerical simulations with the BECs. The result is shown in Fig. 5. Similar to the classical situation, BECs have also been focused by the Gaussian beam. Their shapes became narrow and the advanced propagation in gravity direction was also observable (not shown in the figure).

III. SETUP AND EXPERIMENTAL RESULTS

Our experimental setup consists of two magneto-optical traps [36]. Up-MOT is a low-velocity intense source MOT (LVIS-MOT), in which atoms are captured directly from

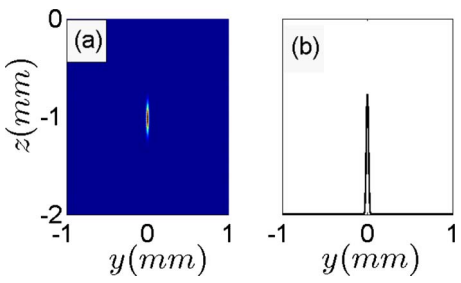

FIG. 5. (Color online) (a) Theoretical imaging of BECs after traversing through the light beam. (b) Corresponding cross section of the BECs along the y axis at the widest of the atomic cloud. Other parameters are the same as in Fig. 2.

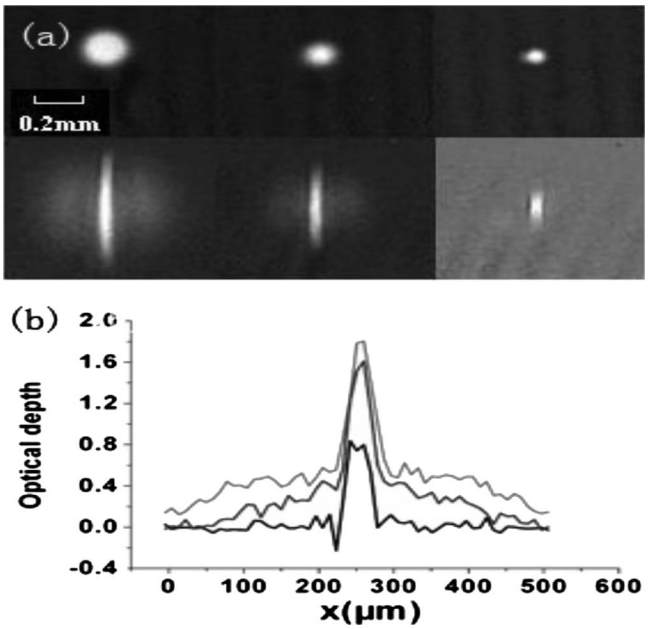

FIG. 6. Results from the experiment. Here, the Rabi frequency is $\Omega_0/2\pi = 100$ MHz, the detuning is $\delta/2\pi = -50$ GHz, and the waist length $w_L = 46$ μm. (a) From left to right, atomic clouds with temperature $T = 1.5$ μK, 480 nK, and less 80 nK, respectively. The flying times of the atomic clouds at the top of Fig. 5(a) are $t = 6$ ms and $t = 16$ ms at the bottom. (b) Cross curves of optical depth. From top to bottom, the temperatures of atomic clouds are $T = 1.5$ μK, 480 nK, less 80 nK, respectively.

atomic vapor. Cold atoms become a slow atomic beam under radiation pressure and are transferred into the second ultrahigh-vacuum MOT (UHV-MOT). About 6×10^8 atoms can be trapped in the UHV-MOT at the best conditions. After the atomic number in the UHV-MOT reached a stable value, we did optical molasses and then loaded atoms into a quadrupole-Ioffe-configuration (QUIC) trap with trapping frequencies of $2\pi \times 210$ Hz in the radial direction and $2\pi \times 21$ Hz in the axial (x) direction. Evaporative cooling of the atoms was performed by rf-induced spin flips. We swept the rf frequency from 25 MHz to a final value of around 1.6 MHz over a period of 28 s. Atomic clouds with various temperatures from about 1 μK to below the transformation point were obtained by setting different final rf frequencies. The cold atomic cloud was then ballistically expanded after the magnetic trap was switched off. The direction of propagation of the focused Gaussian beam and the probing beam was parallel to the long axis of the QUIC trap. Therefore, both cold atomic clouds and BECs were symmetrically distributed in the probing plane before traversing the Gaussian beam. We acquired the distribution of atomic clouds from absorption images, as shown in Fig. 6(a). The waist size was $w_0 \approx 46$ μm and the Rayleigh length was about 8.5 mm. Since the Rayleigh length was far longer than the scale of the atomic cloud while it was passing the light beam, we could approximate that the laser beam provided a two-dimensional Gaussian potential. The power of the focused Gaussian light beam was between $40 \sim 45$ μw with a red detuning $\delta/2\pi = -40 \sim -80$ GHz. When evaporative cooling was finished, we released the BEC from the QUIC trap and turned on the

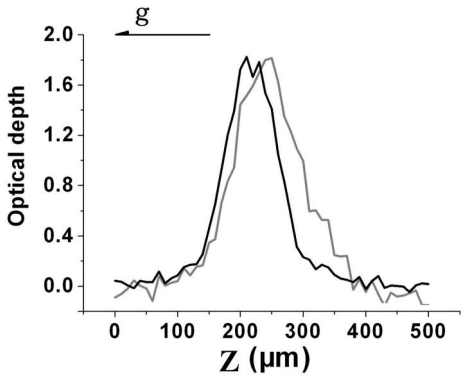

FIG. 7. Advance phenomena along the motion direction. The black line indicates the phenomena with the Gaussian beam and the gray line represents the phenomena without it.

Gaussian beam. After the atomic cloud had passed through it, we turned off the Gaussian beam and waited for several milliseconds. All information regarding the atomic cloud were derived from the absorption images.

Figure 6(a) is a typical experimental result about atomic clouds passing through the red-detuned Gaussian beam. In this experiment, the focused Gaussian beam overlapped in the center of the atomic cloud while it was being released from the QUIC trap at 7 ms. The top pictures in Fig. 6(a) show the symmetric distribution of cold atomic clouds and BECs before they passed through the Gaussian beam. The bottom pictures in Fig. 6(a) show the distribution after they had passed through it. Their flying times were 6 and 16 ms, respectively. There were focused and unfocused parts in the atomic clouds. The ratio of focused parts increases with the decrease in temperature. Figure 6(b) is the cross curve of the optical depth along y axis at the widest part of the atomic cloud. With the dropping of the temperature, the scale of the atomic clouds reduces. After the transition from the gas phase to the Bose-Einstein condensed phase has occurred, we can only find the focused peak.

After passing through the red-detuned Gaussian beam, aside from being focused, the atomic clouds advanced along the motion direction (gravity direction). Figure 7 is the comparison between with and without the red-detuned Gaussian beam. We can see an obvious advanced motion. In this picture, the atomic cloud is a BEC. In fact, advance phenomena still exist when an atomic cloud's temperature is higher than the phase transition point. However, the small scale of BECs makes this effect more easily observable. We have measured the advanced value versus the flying time after the atomic clouds have passed through the Gaussian beam. Before passing through the Gaussian beam, the BECs have already flown 4 ms. They then fly $8 \sim 14$ ms after passing through it. The advanced values are between $37 \sim 44$ μm.

One-dimension cooling phenomenon has also been observed. We have analyzed images in different flying times after cold atomic clouds have been focused. The one-dimension temperature along y axis of the focused part is below 120 nK. In comparison, the background temperature without dipole potential is 660 ± 20 nK. No obvious change of temperature was observed in the other two dimensions.

We have also measured the ratio of focused parts to the entire atomic clouds. Since the Rayleigh length of the laser beam is far longer than the scale of atomic clouds, K is relative to the action length of the Gaussian beam to atoms in the transverse direction. Assuming the atomic cloud's density is a Gaussian distribution with a standard deviation σ_{atom} when it passes through the laser beam and the effective scattering region for atoms is also a Gaussian profile in the y direction with a standard deviation σ_{dipole}, the total atomic number can be expressed as

$$N = \int_{-\infty}^{\infty} n(0) e^{-y^2/2\sigma_{\text{atom}}^2} dy = \sqrt{2\pi} n(0) \sigma_{\text{atom}}. \tag{3}$$

The number of scattered atoms is

$$N_{sca} = \int_{-\infty}^{\infty} n(0) e^{-y^2/2\sigma_{\text{atom}}^2} e^{-y^2/2\sigma_{\text{dipole}}^2} dy$$

$$= \sqrt{2\pi} n(0) \frac{\sigma_{\text{atom}} \sigma_{\text{dipole}}}{\sqrt{\sigma_{\text{atom}}^2 + \sigma_{\text{dipole}}^2}}. \tag{4}$$

Therefore, the ratio of focused part to the entire atomic cloud is

$$K = \frac{N_{sca}}{N} = \frac{\sigma_{\text{atom}} \sigma_{\text{dipole}}}{\sqrt{\sigma_{\text{atom}}^2 + \sigma_{\text{dipole}}^2}}. \tag{5}$$

The action length of the Gaussian beam to atoms is

$$\sigma_{\text{dipole}} = \frac{K \sigma_{\text{atom}}}{\sqrt{1 - K^2}}. \tag{6}$$

Obtaining σ_{atom} and K from experiments, we figure out the action length. Since the total scattering cross section of the Gaussian beam to atoms is in direct proportion to U_0^2/p^2, where momentum $p=mv$, the σ_{dipole} is in direct proportion to U_0/v.

Figure 8 shows the σ_{dipole} versus the corresponding U_0/v. Many parameters, such as the atomic clouds' temperature, the Gaussian beam's time of passing, and the intensity and detuning of the Gaussian beam, have changed in the experiments. However, the linear relationship of σ_{dipole} vs U_0/v is still valid.

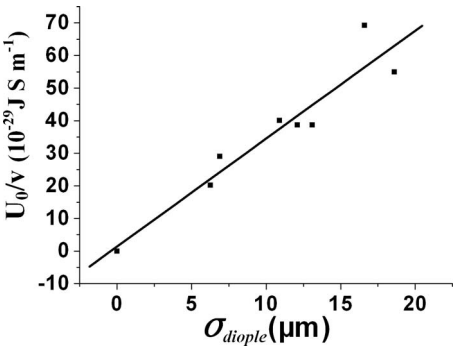

FIG. 8. σ_{dipole} vs corresponding U_0/v.

IV. CONCLUSION

In conclusion, we have studied some phenomena of an atomic cloud traversing a red-detuning Gaussian laser beam,

such as focusing and advance propagation. Based on the model of an atomic cloud traversing a far red-detuned Gaussian light beam, we performed numerical simulations via the DSMC method for the thermal atom cloud and the nonlinear Schrödinger equation for the BECs wave packet, respectively. The numerical results were consistent with those in the experiments.

Abundant phenomena of atom optics were exhibited directly. A Gaussian beam with a small diameter can focus atomic clouds within a short distance. This indicates that a Gaussian beam is an effective element in the study of both coherent and incoherent atom optics. It is a method for obtaining ultracold atomic beams. However, some interesting problems, such as transverse cooling, should be studied further.

ACKNOWLEDGMENTS

This work in SIOM was supported by the National Fundamental Research Program of China under Grant No. 2006CB921202, the National Natural Science Foundation of China under Grant No. 10804115, and the Knowledge Innovation Program of the Chinese Academy of Sciences. W.Z. acknowledges the support of the National Natural Science Foundation of China under Grant No. 10588402, the National Basic Research Program of China (973 Program) under Grant No. 2006CB921104, the Program of Shanghai Subject Chief Scientist under Grant No. 08XD14017, the Program for Changjiang Scholars and Innovative Research Team in the University, Shanghai Leading Academic Discipline Project under Grant No. B480. We also thank Dr. Jun Qian for his invaluable assistance.

[1] C. Monroe, W. Swann, H. Robinson, and C. Wieman, Phys. Rev. Lett. **65**, 1571 (1990).
[2] M. H. Anderson *et al.*, Science **269**, 198 (1995).
[3] T. Esslinger, I. Bloch, and T. W. Hänsch, Phys. Rev. A **58**, R2664 (1998).
[4] P. Meystre, *Atom Optics* (Springer-Verlag, New York, 2001).
[5] C. S. Adams, M. Sigel, and J. Mynek, Phys. Rep. **240**, 143 (1994).
[6] M. R. Andrews *et al.*, Science **275**, 637 (1997).
[7] A. S. Arnold, C. MacCormick, and M. G. Boshier, J. Phys. B **37**, 485 (2004).
[8] Y. B. Ovchinnikov, J. H. Müller, M. R. Doery, E. J. D. Vredenbregt, K. Helmerson, S. L. Rolston, and W. D. Phillips, Phys. Rev. Lett. **83**, 284 (1999).
[9] A. M. Ishkhanyan, Phys. Rev. A **61**, 063611 (2000).
[10] E. A. Cornell, C. Monroe, and C. E. Wieman, Phys. Rev. Lett. **67**, 2439 (1991).
[11] I. Bloch, M. Köhl, M. Greiner, T. W. Hänsch, and T. Esslinger, Phys. Rev. Lett. **87**, 030401 (2001).
[12] A. S. Arnold, C. MacCormick, and M. G. Boshier, Phys. Rev. A **65**, 031601(R) (2002).
[13] M. J. Pritchard, A. S. Arnold, D. A. Smith, and I. G. Hughes, J. Phys. B **37**, 4435 (2004).
[14] S. Choi and K. Burnett, Phys. Rev. A **56**, 3825 (1997).
[15] J. E. Bjorkholm, R. R. Freeman, A. Ashkin, and D. B. Pearson, Phys. Rev. Lett. **41**, 1361 (1978).
[16] J. E. Bjorkholm, R. R. Freeman, A. Ashkin, and D. B. Pearson, Opt. Lett. **5**, 111 (1980).
[17] J. Yin, W. Gao, and Y. Zhu, Prog. Opt. **45**, 119 (2003).
[18] G. M. Gallatin and P. L. Gould, J. Opt. Soc. Am. B **8**, 502 (1991).
[19] L. E. Helseth, Phys. Rev. A **66**, 053609 (2002).
[20] V. I. Balykin, V. S. Letokhov, Yu. B. Ovchinnikov, and A. I. Sidorov, Phys. Rev. Lett. **60**, 2137 (1988).
[21] P. J. Martin, B. G. Oldaker, A. H. Miklich, and D. E. Pritchard, Phys. Rev. Lett. **60**, 515 (1988).
[22] V. I. Balykin, V. S. Letokhov, and A. I. Sidorov, JETP Lett. **43**, 217 (1986).
[23] V. I. Balykin *et al.*, J. Mod. Opt. **35**, 17 (1988).
[24] H. Ito, K. Yamamoto, A. Takamizawa, H. Kashiwagi, and T. Yatsui, J. Opt. A, Pure Appl. Opt. **8**, S153 (2006).
[25] V. I. Balykin and V. G. Minogin, Phys. Rev. A **77**, 013601 (2008).
[26] J. L. Cohen, B. Dubetsky, and P. R. Berman, Phys. Rev. A **60**, 4886 (1999).
[27] B. Rohwedder and M. Orszag, Phys. Rev. A **54**, 5076 (1996).
[28] B. Dubetsky and P. R. Berman, Phys. Rev. A **58**, 2413 (1998).
[29] D. R. Murray and P. Öhberg, J. Phys. B **38**, 1227 (2005).
[30] P. Barberis and B. Rohwedder, Phys. Rev. A **67**, 033604 (2003).
[31] O. Steuernagel, Phys. Rev. A **79**, 013421 (2009).
[32] J. L. Cohen, B. Dubetsky, and P. R. Berman, Phys. Rev. A **60**, 3982 (1999).
[33] L. Fallani, F. S. Cataliotti, J. Catani, C. Fort, M. Modugno, M. Zawada, and M. Inguscio, Phys. Rev. Lett. **91**, 240405 (2003).
[34] L. Pruvost, D. Marescaux, O. Houde, and H. T. Duong, Opt. Commun. **166**, 199 (1999).
[35] G. A. Bird, *Molecular Gas Dynamics and the Direct Simulation of Gas Flow* (Clarendon, Oxford, 1994).
[36] Y. Z. Wang, S. Y. Zhou, Q. Long, S. Y. Zhou, and H. X. Fu, Chin. Phys. Lett. **20**, 799 (2003).